NOTES

Barth's felspar geothermometer: a rapid method

By

P. H. Banham

(Department of Geology, Bedford College, London N.W. 1)

INTRODUCTION

The use of the felspar geothermometer (Barth 1956, 1961, 1962) for the purpose of estimating the temperature of crystallization of two-felspar rocks depends on the determination of the albite content of both the alkali and plagioclase felspars. Each of these determinations is beset with difficulties, however. The alkali-felspar is frequently perthitic (often possibly a secondary condition), and, unless previously homogenized by heating at temperatures up to 900°C (Tuttle and Bowen 1958, pp. 13 seq.), it is very difficult to separate from the whole rock sample for wet chemical or X-ray analysis. The plagioclase composition may sometimes be reliably determined by optical methods. However, secondary alteration, at least to fine-grained 'saussurite' minerals, is common, and, as this will have increased the albite content of the remaining plagioclase, a minimum figure only will be determined for the temperature of crystallization.

The method described attempts to overcome these difficulties; only the results of mineral modal and wet chemical analyses are required.

PRINCIPLE OF THE METHOD

Two sets of data are required:

1) A modal analysis of the rock in which the proportions of plagioclase and alkali-felspar are expressed as percentages of total felspar.

2) A chemical analysis of total felspar of the rock, re-calculated and expressed as percentages of the ideal felspar molecules: Or, Ab, and An (here referred to as the felspar 'norms'). Alteration products of

both felspars should be treated as felspar during the above procedures, provided that such alteration is slight, fine-grained, and iso-chemical.

Modal alkali-felspar will exceed the Or norm by the amount of albite contained by the alkali-felspar. This difference may be deducted from the Ab norm and the remainder of the latter, when taken with the An norm, will give the Ab: An ratio of the plagioclase. Using these values, the albite partition coefficient may be simply calculated. (The An content of alkali-felspar, and, likewise, the Or content of the plagioclase, may reasonably be supposed to be of the same order, low and of negligible significance for this method. See also ORVILLE 1962, p. 344.)

EXAMPLE OF THE METHOD

A granite from the Hestbrepiggan area of the N.W. Basal Gneiss Area of southern Norway (BANHAM and ELLIOTT 1965, BANHAM 1966) is used for the purpose of illustration. The method may conveniently be divided into three stages:

1) *Microscope work.* An accurate modal analysis of the rock is prepared, using the methods of CHAYES (1956):

Quartz	32%
Biotite	7%
Alkali-felspar	41% (67% of total felspar)
Plagioclase	20% (33% of total felspar)

2) *Chemical work.* To obtain the normative felspar proportions it is not necessary to separate individual rock felspars, or even total felspar, as pure samples. An optically pure mixture of felspars and quartz may be used. This can readily be obtained by the simple separation of the powdered rock sample into a heavy (and electromagnetic) fraction, consisting only of biotite in this case, and a light (and relatively non-electromagnetic) fraction consisting of the required felspar plus quartz mixture. Normally, very few runs through an electromagnetic separator are required for a good separation.

The felspar and quartz mixture is then chemically analysed; the rapid methods of SHAPIRO and BRANNOCK (1952, 1956) have been used in this case. Theoretically, only the values of Na_2O, K_2O, and CaO are necessary for the subsequent felspar recalculation. (Where the plagioclase felspar is unaltered and its Ab:An ratio determinable by

optical methods, only the Na_2O (or K_2O) figure need be determined here.) However, the Al_2O_3 and SiO_2 values provide additional checks on the calculation, and a complete analysis is recommended as a purity and accuracy check.

The oxide percentages determined are re-expressed as cation percentages, and from these the proportions of the Or, Ab, and An norms may be calculated, using the ideal formulae. A large overall excess of Si of course reflects the presence of abundant quartz in the sample. A slight excess of Al is usual and is probably consequent on slight alteration and/or leaching of the felspars. It might represent some more fundamental substitution in the felspars themselves, however; for example, Al for Si in the tetrahedral sites.

In this case, the recalculated felspar norm proportions are:

$$\text{Or} - 50.9\% \; ; \quad \text{Ab} - 41.2\% \; ; \quad \text{An} - 7.9\%.$$

3) *Interpretation of the results.* Modal alkali-felspar exceeds the Or norm by the amount of albite contained by the alkali-felspar, i.e. 16.1%; thus, the albite proportion of alkali-felspar is *24*% (16.1/67.0).

The amount of the Ab norm allotted to alkali-felspar may now be deducted from (total) Ab norm to leave only the amount of Ab contained by the plagioclase-felspar (41.2% − 16.1% = 25.1%). Thus, the proportion of albite in plagioclase is *76*% (25.1/25.1 + 7.9).

The albite partition coefficient K may now be determined:
Ab in alkali-felspar: Ab in plagioclase-felspar

$$K = 24 : 76 = .316$$

Using the data given by BARTH (1962, Figs. 3 and 4), the temperature of crystallization of this granite is 590°C (approximately). (This is likely to be a minimum for a small quantity of epidote after plagioclase has probably been lost from the felspar sample during electromagnetic separation.)

CONCLUSIONS

The method described is rapid, requires no special skills or apparatus, and many samples may be cheaply determined. Further, this method is thought to be at least as accurate and significant as those that depend upon homogenization and/or fine grinding and extremely laborious, yet imperfect, felspar separations.

ACKNOWLEDGEMENTS

This method of felspar geothermometry was evolved at Nottingham University during the writer's tenure of a DSIR/NATO Research Studentship (1959–1962) in the Department of Geology. Particular thanks are due to Dr. R. B. Elliott of that department, who extensively criticized the manuscript of this paper.

Professor Tom. F. W. Barth also very kindly read the final manuscript and suggested certain modifications.

REFERENCES CITED

BANHAM, P. H. 1966. Fault vein mineralization as the result of shearing in Norwegian basement rocks. Norsk geol. tidsskr. 46: 181–191.

BANHAM, P. H. and ELLIOTT, R. B. 1965. Geology of the Hestbrepiggan area: Preliminary account. Norsk geol. tidsskr. 45: 189–198.

BARTH, T. F. W. 1956. Studies in gneiss and granite I and II. Skr. Norske Vid.-Akad. Oslo. I. Mat.-Naturv. Kl. 1956, No. 1: 1–32.

— 1961. The felspar lattices as solvents of foreign ions. Inst. Lucas Mallada Cursillos y Conferencias. Fasc. 8. 3 pp.

— 1962. The feldspar geologic thermometers. Norsk geol. tidsskr. 42 (Feldspar volume): 330–339.

CHAYES, F. 1956. Petrographic modal analysis. Wiley & Sons., Inc., New York.

ORVILLE, P. M. 1962. Comments on the two-felspar geothermometer. Norsk geol. tidsskr. 42 (Felspar volume): 340–346.

SHAPIRO, L. and BRANNOCK, W. W. 1952. Rapid analysis of silicate rocks. Geol. Surv. America Circ. 165.

— 1956. Rapid analysis of silicate, rocks (A contribution to geochemistry) Geol. Surv. America Bull. 1036–C (Circ. 165 revised).

TUTTLE, O. F. and BOWEN, N. L. 1958. The origin of granite in the light of experimental studies. Geol. Soc. America Mem. 74: 1–153.

Accepted for publication February 1966

Exaggerated grain growth in the metamorphism of monomineralic rocks

By

Harald Carstens

(Norges Geologiske Undersökelse, Postboks 3006, Trondheim)

Abstract. It is shown that porphyroblasts in dunites, dolomites, and anorthosites formed during metamorphism by exaggerated grain growth. Normal grain-growth inhibiting factors are accessory constituents, oriented structures, and annealing twins.

According to the traditional metallurgical and more recent ceramic and mineralogic usage, recrystallization is the process by which a new generation of essentially strain-free grains grow at the expense of the originally badly deformed crystals. Grain growth is the increase of grain-size during metamorphism; the driving force is the interfacial free energy. Buerger and Washken (1947) pointed out that the metamorphism of monomineralic rocks usually takes place by recrystallization and grain growth in the solid state. Dunites, anorthosites, limestones, and quartzites commonly show distinct signs of grain growth, as demonstrated by Voll (1960). Vernon (1965) described grain growth phenomena of plagioclase in mafic gneisses. Stanton (1964) showed that metamorphic ores consisting of single-phase aggregates of either pyrite, pyrrhotite, sphalerite, or galena have grown according to the same principles. By normal grain growth, the average size of the grains increases, and the size of the individual grains is fairly uniform. If, on the other hand, a small fraction of the grains attains a large size by growing more rapidly than others, the process is called exaggerated (abnormal, discontinuous) grain growth (see e.g. Hillert 1965). It is the purpose of the present note to draw attention to porphyroblastic structures in monomineralic rocks indicative of exaggerated grain growth.

An area of dunite at Åheim, Sunnmöre in West Norway, contains a number of nearly spherical monocrystals of olivine varying in size

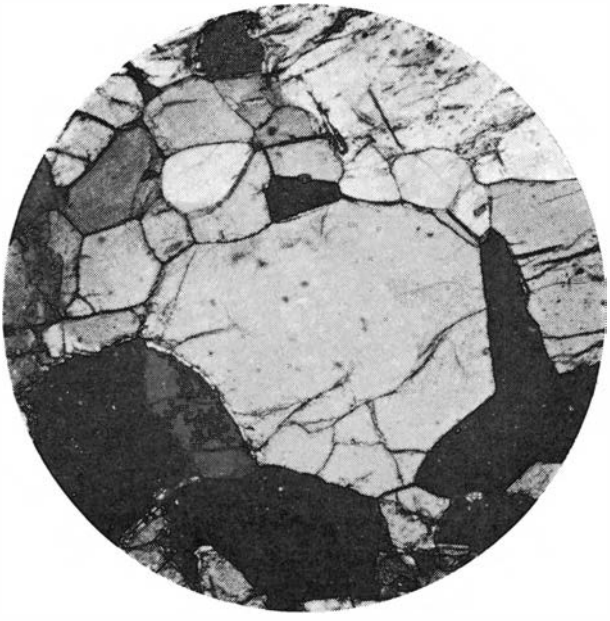

Fig. 1. Exaggerated grain growth in dunite. The central large grain having thirteen sides has grown by the migration of its boundaries towards their centres of curvature. The black grains are olivine in extinction position. The composition of the small and the large olivine crystals is about Fo 12. Nicols +. × 29.

from about 1 mm up to 15–20 mm. The average grain size of the matrix is 0.5–1 mm. In stream gravel of the dunite area, similar olivine crystals, about 10 cm in diameter, have been found. The dunite contains small amounts of chlorite, diopside, tremolite, and iron ores. The fact that the angles between olivine grain boundaries are usually about 120 degrees is attributed to nearly isotropic grain boundary energy. Most boundaries are curved, the large grains always having convex boundaries when observed from the inside (Fig. 1). Olivine/olivine boundaries are commonly perpendicular to the basal plane of chlorite, demonstrating a high dihedral angle and high interfacial energy of the boundary between olivine and the 001-plane of chlorite. This may be an important factor in preventing normal grain growth during metamorphism (Voll 1960).

Exaggerated grain growth has been obtained experimentally in annealed calcite aggregates (Griggs *et al.* 1960). Similar porphyro-

blasts are sometimes observed in the dolomites of North Norway, although the structures are not so spectacular as in the dunites. The equilibrium angles at triple junctions and the convex boundaries of the large grains indicate the nature of the porphyroblasts. The matrix, as well as the large grains, is completely unstrained, both in the dolomite and the dunite, so the growth is in no way related to strain-induced boundary migration.

The theoretical basis for the understanding of normal and exaggerated grain growth in metamorphic rocks is the result of work done in metallic and ceramic systems (BURKE and TURNBULL 1952, BURKE 1959). It has been shown that the rate of grain boundary movement during grain growth is inversely proportional to the radius of the curvature of the boundary, or, in other words, inversely proportional to the average grain size: $dD/dt = K/D$, where D is the average diameter of the grains. In principle, therefore, if time does not put an end to the growth as in many geological processes, grain growth will continue until a single-phase polycrystalline rock becomes a single giant crystal. Such rocks do not exist, because in addition to the diminishing rate of growth as time progresses — approaching zero — there is usually a limiting grain size due to the presence of other minerals (or pores) which may inhibit grain growth. Normal grain growth stops when $D = d/f$, where D again is the average diameter of the grains, d the average diameter of the inclusions, and f the volume fraction of the inclusions. Evidence of the impeding effect of mineral inclusions is offered by VOGT (1940), who demonstrated that the grain size of metamorphic pelitic rocks in the Trondheim area decreases with increasing content of carbonaceous matter. The ability of small amounts of graphite to restrict grain growth has been confirmed experimentally in hot-pressed BeO (LANGROD 1965). Other examples of grain-growth inhibiting inclusions in metamorphic rocks are given by VOLL (1960). It appears that a prerequisite for the occurrence of exaggerated grain growth in metallic and ceramic systems is the presence of inclusions or pores. Because the growth force is proportional to $N = 6$, where N is the number of sides of the grains, a large grain, which for topological reasons has more sides and more curved boundaries, may be able to grow past the impurities. This grain then consumes its smaller neighbours, the boundaries of which are locked by the inclusions. As monomineralic rocks are never strictly single-phased, but contain accessory

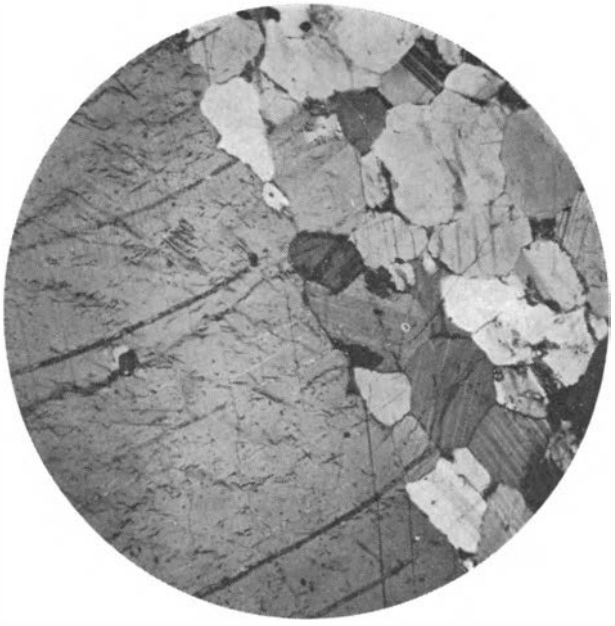

Fig. 2. Porphyroblast of plagioclase in anorthosite. The composition of the small grains is similar to the large one and about An 43. The twins are probably annealing twins, that is to say they originated by grain growth. Some potash feldspar commonly occurs along grain boundaries, especially at triple junctions. Nicols +. × 22.

constituents of various kinds, the above explanation may also apply to natural rocks. An additional factor may be the effect of an oriented metamorphic structure. The Åheim dunite is slightly foliated and contains lattice-oriented olivine grains (PHILLIPS 1938). This implies the presence of low-energy boundaries of low mobility and a grain which is differently oriented from the majority will grow more easily. Similarly, an inhomogeneous distribution of accessories which assume the role of grain-growth inhibitors may explain some cases of grain growth, especially in the absence of engulfed accessories in the interior of the large grains.

As expected from the grain boundary energy model, the shape of the porphyroblasts formed by exaggerated grain growth is more or less spherical (Fig. 1). Porphyroblasts of plagioclase in the anorthosite of the Egersund region, which in all likelihood are formed by exagger-

ated grain growth, commonly appear to have an idiomorphic outline. The boundaries, however, are not perfectly straight, but form grooves at the intersections with the boundaries of the smaller grains (Fig. 2) showing adjustment to equilibrium angles. Twinning according to the albite law is very common. Following an argument proposed by FULLMAN and FISCHER (1951) that 'annealing twins may form during grain growth when the free energy of the boundaries between a grain's neighbours and its twin would be less than that of the boundaries between the neighbours and the grain itself', it may be suggested that this reduction in the total interfacial free energy (the driving force for grain growth) might be an important restriction to grain growth in anorthosites. Euhedral porphyroblasts of gypsum in fine-grained gypsum are frequently observed (GRIGOR'EV 1965). Straight boundaries over large distances may, theoretically at least, be explained in terms of anisotropic grain boundary energy. A more likely solution to the problem, explaining euhedral exaggerated grain growth in some ceramic systems, may according to KOOY (1962) lie in the presence of a fluid phase having a small dihedral angle. Grain growth may then take place by a solution and precipitation process, and the grains will display the euhedral shape characteristic of minerals solidified from the melt.

It is probable that exaggerated grain growth frequently occasions porphyroblastesis in metamorphic monomineralic rocks. Is not the porphyroblastic structure observed in metamorphic evaporites sometimes the result of such processes? However, there is a definite need for experimental studies to find out what controls grain growth phenomena in natural rocks.

REFERENCES

BUERGER, M. J. and WASHKEN, E. 1947. Metamorphism of minerals. Am. Mineralogist 32: 296–308.

BURKE, J. E. 1959. Grain growth in ceramics. *In* Kinetics of high temperature processes. New York, pp. 109–116.

BURKE, J. E. and TURNBULL, D. 1952. Recrystallization and grain growth. Progress in metal physics 3: 220–292.

FULLMAN, R. L. and FISCHER, F. C. 1951. Formation of annealing twins during grain growth. Jour. Appl. Phys. 22: 1350–1355.

GRIGGS, D. T., PATERSON, M. S., HEARD, H. C. and TURNER, F. J. 1960. Annealing recrystallization in calcite crystals and aggregates. Geol. Soc. America Mem. 79: 21–37.

GRIGOR'EV, D. P. 1965. Ontogeny of minerals. Jerusalem, pp. 1–250.

HILLERTS, M. 1965. On the theory of normal and abnormal grain growth. Acta Met. 13.

KOOY, C. 1962. Anisotropic exaggerated grain growth and sintering in $MnFe_2O_4$ and $Y_3Fe_5O_{12}$. Science of ceramics 1: 21–34.

LANGROD, K. 1965. Graphite as grain growth inhibitor in hot-pressed beryllium oxide. Jour. Am. Ceram. Soc. 48: 110–111.

PHILLIPS, F. G. 1938. Mineral orientation in some olivine-rich rocks from Rum and Skye. Geol. Mag. 75: 130–135.

STANTON, R. L. 1964: Mineral interfaces in stratiform ores. Inst. Min. and Met. Bull. 64: 45–79.

VERNON, R. H. 1965. Plagioclase twins in some mafic gneisses from Broken Hill, Australia. Mineralog. Mag. 35: 448–507.

VOGT, TH. 1940. Geological notes on the Dictyonema locality and the upper Guldal district in the Trondheim area. Norsk geol. tidsskr. 20: 171–191.

VOLL, G. 1960. New work on petrofabrics. Liverpool and Manchester Geol. Jour. 2: 503–567.

Accepted for publication February 1966

A note on the interpenetration of detrital quartz grains during the formation of sedimentary quartzites

BY

HARALD CARSTENS

(Norges Geologiske Undersökelse, Postboks 3006, Trondheim)

Abstract. It is suggested that contrasting degrees of quartz interpenetration in a small sample of sediment are due to non-uniform wetting of the grains by pore water.

Compaction of sand grains because of increasing pressure occasioned by burial results in a volume reduction of the sediments. Slight burial tends to rearrange the sand grains to give higher packing density and lower pore volume resulting in a permeable sandstone in which the quartz grains have mutual, tangential contacts. This is achieved by the grains sliding over one another. With increasing depth of burial,

processes occur which decrease the centre-to-centre distances between grains allowing further reduction in volume. Tangential contacts are thereby progressively replaced by interlocking boundaries described as long, concavo-convex, and sutured (stylolitic) showing increasing

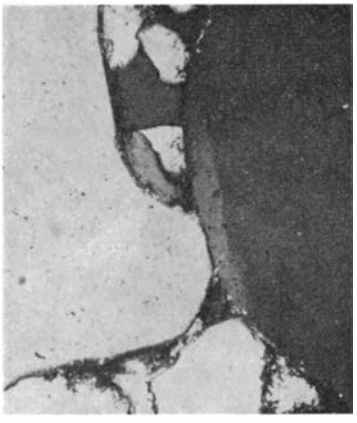

Fig. 1. Strain in quartz at points of grain contact. × 122.5.

Fig. 2. Recrystallization of quartz related to strained contacts. × 122.5.

degrees of interpenetration. This process may proceed to a stage where individual grains eventually loose their identity. Thus, destruction of the primary point-to-point contacts ultimately results in a quartzite with little or no cement. In contrast to the orthoquartzite which contains essential amounts of cementing quartz, this type of sedimentary quartzite has been termed pressolved quartzite (SKOLNICK 1965). The name is derived from the process believed to be involved in the interpenetration of quartz grains. It is generally agreed that sintering occurs by transfer of material from points of contact because of compressive stress, the driving force being the increased chemical potential at the contacts.

There is, however, no consistent, unequivocal relationship between depth of burial and interpenetration boundaries, and sometimes all kinds of contacts are found in the same thin section. A quartz grain may, for example, have deeply interpenetrated boundaries on one side and tangential contacts on the opposite. A close inspection of tangential contacts associated with interpenetration boundaries discloses that those parts of the grains that are adjacent to the point contacts are

strained. A number of observations[1] show that undulatory extinction in the quartz grains is related to stress at these contacts. (Fig. 1). It may also be inferred that the strain level reached a considerable magnitude because the strained quartz has often recrystallized (Fig. 2). No crushing or fracturing of the quartz grains which occur in experimentally compacted sands (MAXWELL 1960) was observed. The important conclusion to be drawn from the above observations is that stress relief at grain contacts variously occurs by pressure solution and plastic deformation. We may now ask why quartz reacts so differently when subjected to stress? A prerequisite for pressure solution to occur is that the grains be separated by a thin water film. Quartz may then go into solution at the stressed contacts and diffuse into open voids and precipitate there or be transported away by percolating water. Thus, if $\gamma_{SS} < 2\gamma_{SL}$,[2] the dihedral angle is zero and the quartz grains form solid-to-solid boundaries, and, because of the slow diffusion in the solid state compared with liquid diffusion, tangential contacts are preserved. Coating on grain surfaces may have a marked influence on the grain-water interfacial energy, which therefore probably varies considerably along the surfaces of detrital quartz grains. Variations in the grain boundary energy (γ_{SS} may, of course, contribute to the wetting ability, but is in all likelihood of little significance.

The catalytic effect of coating material (LERBEKMO and PLATT 1962) in the pressure-solution of quartz is another factor which may accentuate the contrasting behaviour of the detrital grains during the diagenesis.

REFERENCES

LERBEKMO, J. F. and PLATT, R. L. 1962. Promotion of pressure-solution of silica in sandstones. Jour. of sedimentary petrology 32: 514–519.

MAXWELL, J. C. 1960. Experiments on compaction and cementation of sand. *In* Rock deformation, Geol. Soc. America Mem. 79: 105–132.

SKOLNICK, H. 1965. The quartzite problem. Jour. of sedimentary petrology 35: 12–21.

Accepted for publication February 1966

[1] The material used in this study, sandstones from the Precambrian of South Norway (Trysil) and sandstones from below the Hyolithes zone of Finnmarken, North Norway, was supplied by state geologists Skålvoll and Gvein.

[2] γ_{SS} = grain boundary energy. γ_{SL} = solid–liquid interfacial energy.

The effect of twinning on the recrystallization of albite

By

Harald Carstens

(Norges Geologiske Undersökelse, Postboks 3006, Trondheim)

Abstract. It is shown that the large strains which accumulate in albite twinned in a chess-board pattern on the albite law may initiate recrystallization of the albite.

It is well known that feldspar, in contradistinction to, for example, calcite and quartz, recrystallizes only with great difficulty. When highly deformed, plagioclase may show incipient recrystallization at grain boundaries or along those parts of the grains which have been reoriented (deformation bands, substructures, etc.) as observed, e.g., in the anorthosites of West Norway. Twinning, likewise, under some circumstances seems to be favourable for the nucleation and growth of strain-free grains. Chess-board albite affords an example of this.

Chess-board albite is characterized by dense arrays of narrow, discontinuous albite lamellae. The twin boundaries are usually stepped or lenticular and commonly terminate abruptly. A high content of incoherent twin boundaries therefore distinguishes the chess-board pattern of twinning.

The origin of chess-board twinning is in dispute. Chess-board albite is often present in quartzo-feldspathic rocks in areas of regional metamorphism in Norway and elsewhere, and, for this reason, it has been suggested (Starkey 1959) that chess-board twinning is a mechanical twinning. Chess-board twinning seems to be confined to rather pure albite (Battey 1955), and it is probable that the difficulties involved in the twinning of ordered low-albite (Laves 1952) may be of importance in controlling the peculiar twinned pattern of this feldspar. Whatever the origin, however, there is a definite tendency for chess-board albite to recrystallize during post-tectonic annealing conditions. The description below pertains to the recrystallization reaction in quartz-keratophyres near Trondheim. Recrystallization starts along the

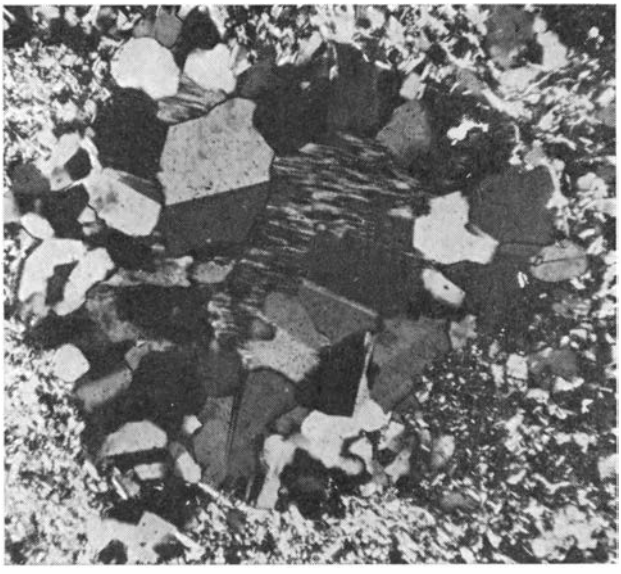

Fig. 1. Recrystallization of chess-board albite in quartz-keratophyre near Trondheim. Crossed nicols, × 145.

boundaries of the chess-board albite and proceeds inwards, eventually replacing the whole crystal by an assemblage of new strain-free grains (Fig. 1). The orientation of the new generation of albite varies, but the majority of the grains have the (010)-plane parallel to (010) of the chess-board albite. Another maximum is found for grains oriented with (010) normal to (010) of the old one. The new grains are either untwinned or simply twinned according to the albite law, the latter being the more usual. The twin plane nearly always penetrates along the middle of the recrystallized grains, thus giving the impression that they started to grow from a twinned nucleus. Grains are of fairly uniform size, about 0.1–0.2 mm in diameter, and they did not grow further after impingement.

The internal energy of albite twinned in a chess-board pattern is considerably higher than that of untwinned albite or albite having normally spaced and coherent twin lamellae. Strain energy is stored along the twin boundaries, especially along those which are incoherent. By an investigation of the mechanism of formation of mechanical

twins in calcite, it has been shown (STARTSEV 1963) that the twinning is accompanied by point defects, stacking faults, and perfect dislocations in addition to the twinning dislocations. Thus, very large strains may be introduced in minerals during the act of twinning. It is this excess energy which is believed to be the driving force for recrystallization in chess-board albite. The author knows of no other example among natural minerals of recrystallization related to twinning. Deformation twinning in calcite does not appear to have any influence on the recrystallization of calcite. Kuznetzov and Kopora (HALL 1954) and others (CAHN 1954), however, have observed recrystallization of zinc crystals along twin boundaries, preferentially at twin intersections.

REFERENCES

BATTEY, M. H. 1955. Alkali metasomatism and petrology of some keratophyres. Geol. Mag. 92: 104–126.

CAHN, R. W. 1954. Twinned crystals. Advances in Physics 3: 363–445.

HALL, E. O. 1954: Twinning and diffusionless transformation in metals. Butterworths, London.

LAVES, F. 1952. Mechanische Zwillingsbildung in Feldspaten in Abhängigkeit von Ordnung-Unordnung der Si/Al-Verteilung innerhalb des $(Si,Al)_4O_8$-Gerüstes. Naturwissenschaften 23: 546–547.

STARKEY, J. 1959. Chess-board albite from New Brunswick, Canada. Geol. Mag. 96: 141–145.

STARTSEV, V. J. 1963: The formation of defects in crystal lattice by twinning. Proc. Int. Conf. Crystal Lattice Defects. Phys. Soc. Japan, 18, Suppl. III: 16–20.

Accepted for publication March 1966

Distribution of some elements among minerals of Norwegian eclogites

By

Y. Matsui, S. Banno, and I. Hernes

(Institute for Thermal Spring Research, Okayama University, Geological Institute, University of Tokyo, and Geological Institute, University of Bergen)

Abstract. Coexisting clinopyroxene, orthopyroxene, and garnet from a lens of eclogitic rocks of Norway are analysed for their Mg, Ni, Co, Zn, Fe, and Mn contents. Examination of their distribution among these three phases reveals that: 1) in the pair orthopyroxene–clinopyroxene, the partition is essentially controlled by the size of the cations, so that, as far as the moderate-sized ions as listed above are concerned (except for Mn), the smaller ions prefer clinopyroxene, and 2) in the pair garnet–clinopyroxene, the partition is controlled by two factors, i.e. that the larger ions prefer garnet and that the less electronegative ions are excluded from garnet.

This note is a preliminary report on the distribution of certain cations among clinopyroxene, orthopyroxene, and garnet in the eclogitic rocks of Norway.

The petrology of the host rocks will be given elsewhere. The rocks are from a lens of eclogitic rocks enclosed in gneiss at Kolmanskog, Molde Peninsula, Norway (Hernes 1954). The major constituents of the rocks are clinopyroxene, garnet, and orthopyroxene together with subordinate hornblende and iron ores. The analysed minerals were separated by conventional methods to obtain a purity higher than 98%.

Chemical analyses were carried out by atomic absorption flame photometry using a Nippon Jarrel-Ash Model AA-1E flame photometer with H_2-air flame for Mn, Co, Ni, Cu, and Zn; by emission flame photometry after the standard addition technique for Ca in orthopyroxene; by chelatometric titration for Ca and Mg, and by colorimetry for Fe. Accuracy has been gauged from the analysis of the standard W-1 using similar techniques. Errors were estimated to be less than 5% relative.

Table 1. *Eclogite No. 2 (contents in ppm)*

	Garnet	Ortho-pyroxene	Clino-pyroxene	K'Gar · Cpx / M · Fe	K'Opx · Cpx / M · Fe
Mg	97,900	186,500	105,000	0.22	0.59
Ca	34,300	3,100	167,000	....	....
Mn	6,400	1,660	800	1.88	0.69
Fe	122,000	85,500	28,500	1.00	1.00
Co	119	177	77	0.36	0.77
Ni.....	28	330	190	0.034	0.58
Cu	1	1	40	....	....
Zn	29	102	30	0.23	1.13

Table 2. *Eclogite No. 3 (contents in ppm)*

	Ortho-pyroxene	Clino-pyroxene	K'Opx · Cpx / M · Fe
Mg	179,400	103,000	0.58
Ca	5,700	163,000	....
Mn	1,800	830	0.73
Fe	90,700	30,400	1.00
Co	196	87	0.76
Ni.....	740	460	0.54
Cu	3	103	....
Zn	117	35	1.12

Results of the analyses are presented in Tables 1 and 2. It is notable that Cu is concentrated almost exclusively in clinopyroxene, suggesting the oxidation state of Cu(I). Therefore, in this case, the oxidation state of Fe can be supposed most plausibly to be + 2.

The apparent partition coefficients are also given in the Tables. They are defined as follows:

$$K' \frac{X \cdot Y}{M \cdot Fe} = (M/Fe)_X / (M/Fe)_Y \qquad (1)$$

where symbols X and Y refer to the silicate phases under consideration and M denotes a divalent ion of the size similar to those of Mg and Fe. This way of presentation of partition coefficient has been discussed

elsewhere (BANNO and MATSUI 1965). In brief, the apparent partition coefficient $K' \frac{X \cdot Y}{M \cdot Fe}$ is approximately equal to the equilibrium constant in the exchange reaction:

$$(M)_X + (Fe)_Y = (Fe)_X + (M)_Y \qquad (2)$$

Since the classical work of GOLDSCHMIDT (1926), it is widely accepted that ionic size plays a fundamental role in the processes of elemental distribution. Hence, it is interesting to see the relation between log K' values, which are approximately proportional to the exchange energies, and relevant ionic radii. Figs. 1 and 2 are such diagrams for the mineral pairs garnet–clinopyroxene and orthopyroxene–clinopyroxene, respectively. Pauling's radii are used in construction of the Figures (PAULING 1927). (The adoption of Pauling's set is a matter of convenience. Actually, choice of Ahrens' set results in little effect upon the trends discussed below.)

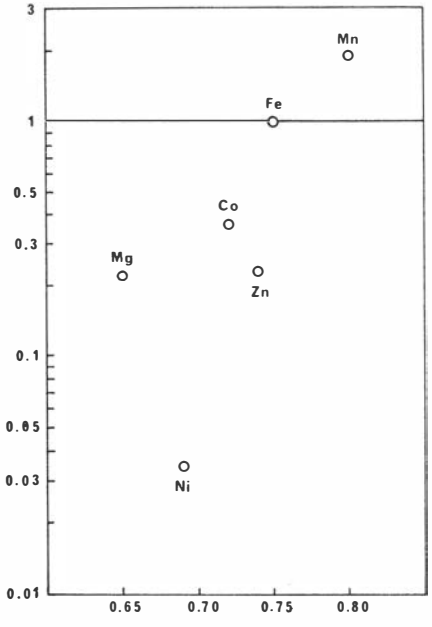

Fig. 1. Distribution pattern between garnet and clinopyroxene. Abscissa: Ionic radius Å. Ordinate: $K' \frac{Gar \cdot Cpx}{M \cdot Fe}$

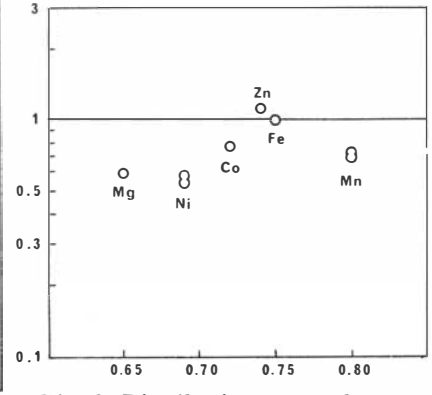

Fig. 2. Distribution pattern between orthopyroxene and clinopyroxene. Abscissa: Ionic radius Å. Ordinate: $K' \frac{Opx \cdot Cpx}{M \cdot Fe}$

In Fig. 1, the relation between log K′ and ionic radius is not so simple. Though there is a general tendency that larger ions prefer garnet, and this can be understood considering the fact that garnet is essentially the mineral of relatively large cations such as Mn, it is obvious that Ni and Zn, and perhaps Co also, deviate from this tendency. As is noticed by some authors (NEUMANN 1949, WEDEPOHL 1953), the geochemical coherence of Zn and Fe is rather weak, despite the similarity in their ionic radii. This phenomenon is usually explained by the difference in their electronegativities or electron affinities. The degrees of deviation from the tentative join Mg–Fe–Mn in Fig. 1 are Ni > Zn > Co. This order coincides with that of their second ionization potentials, viz., Ni: 18.147, Zn: 17.959, and Co: 17.052 (in eV) (AHRENS 1964).

In contrast to the above pair, the pattern of partition between ortho- and clinopyroxenes (Fig. 2) is far more regular. The fact that the join Ni–Co–Fe is shifted to the right as compared to the join Mg–Zn is most probably due to the apparent shrinkage of the ionic size of the former group according to the crystal-field effect (CURTIS 1964). [Note, for example, that the lattice dimensions of $CaNiSi_2O_6$ are smaller than those of $CaMgSi_2O_6$ (GJESSING 1941).] Thus, in this pair it can be said that the smaller ions prefer clinopyroxenes. This is explained qualitatively as the mean size of the sites for cations of moderate size, i.e. exchangeable with Mg and Fe, is smaller in clinopyroxene than in orthopyroxene, which has large M_1 sites (GHOSE 1965). The departure of Mn is possibly due to the replacement of Mn for Ca in clinopyroxene.

As a conclusion, the following statement can be made: the partition of cations between minerals of similar anionic characters (such as ortho- and clinopyroxenes) is controlled by the size of cations irrespective of their chemical properties; this holds for both major and trace elements. The partition between minerals of different anionic characters is more complicated and reflects the type of individual chemical bonds. This sort of statement is, in fact, not novel. Nevertheless, we should like to emphasize that our conclusion has been derived purely from the analysis of the partition of the elements between coexisting minerals.

REFERENCES

AHRENS, L. H. 1964. The significance of the chemical bond for controlling the geochemical distribution of the elements — Part 1. *In* Ahrens, L. H., Press, F., and Runcorn, S. K. Editors, Physics and chemistry of the earth, Vol. 5: 1–54. Pergamon Press, Oxford.

BANNO, S. and MATSUI, Y. 1965. Eclogite types and partition of Mg, Fe, and Mn between clinopyroxene and garnet. Proc. Japan Acad. 41: 716–21.

CURTIS, C. D. 1964. Applications of the crystal-field theory to the inclusion of trace transition elements in minerals during magmatic differentiation. Geochim. et Cosmochim. Acta 28: 389–403.

GHOSE, S. 1965. Mg^{2+}–Fe^{2+} order in an orthopyroxene, $Mg_{0.93}Fe_{1.07}Si_2O_6$. Zeit. Krist. 122: 81–99.

GJESSING, L. 1941. Contribution a l'étude des métasilicates. Norsk geol. tidsskr. 20: 265–67.

GOLDSCHMIDT, V. M. 1926. Geochemische Verteilungsgesetze der Elemente. VII Die Gesetze der Krystallochemie. Skr. Norske Vid.-Akad. Oslo. I. Mat.-Naturv. Kl. 1926. No. 2.

HERNES, I. 1954. Eclogite-amphibolite on the Molde peninsula, Southern Norway. Norsk geol. tidsskr. 33: 163–184.

NEUMANN, H. 1949. Notes on the mineralogy and geochemistry of zinc. Mineral. Mag. 28: 575–581.

PAULING, L. 1927. The sizes of ions and the structure of ionic crystals. Jour. Am. Chem. Soc. 49: 765–790.

WEDEPOHL, K. H. 1953. Untersuchungen zur Geochemie des Zinks. Geochim. et Cosmochim. Acta 3: 93–142.

Accepted for publication April 1966

Curved joints in gneiss

BY

IVAR OFTEDAL

In aerial photographs of the island of Justöy, on the Norwegian Skagerrack coast south of Lillesand, a pattern of long, almost rectilinear joints is a highly predominant feature (Fig. 1). The majority of them are very nearly vertical and at right angles to the main schistosity plane of the gneiss (OFTEDAL 1956), i.e. directed with minor deviations

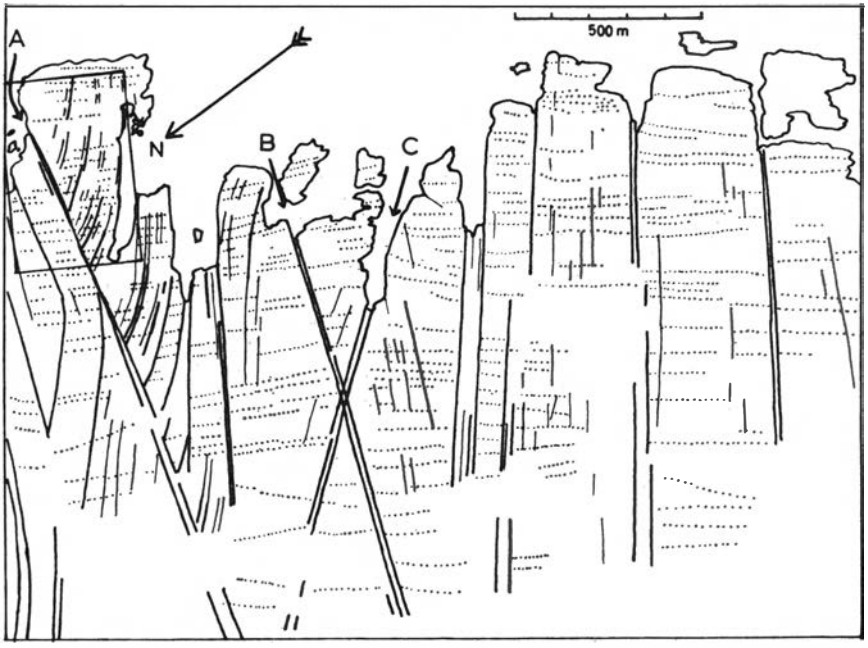

Fig. 1. Part of Justöy. Vertical joints (full lines) and ridges, etc. along the strike (dotted lines). Heavy lines indicate joints which are morphologically predominant. (See also Fig. 4.)

towards E 35°S. In the field, it can be seen that the joints belonging to this quasi-parallel set are much more numerous than appears from the aerial photographs; in fact, neighbouring joints are often about 1 m, or even less, apart. (Fig. 2) Vertical rock walls due to some of these joints show the presence of other sets of joints — one apparently horizontal and one dipping steeply landwards (about W 35°N) (Fig. 3). As the outcrops of the latter must be approximately parallel to the strike, they are not morphologically conspicuous. The gneiss, which accounts for nearly all of the country rock, is mechanically massive; it does not easily split along schistosity planes. It seems natural to interpret all of these joints as pure tension cracks.

There are some joints of a different kind. A few of them are highly conspicuous, having given rise to narrow clefts and valleys. They are nearly straight and form angles of about 20° with the vertical joints of the above set (Fig. 1, A, B, C). They are very long, and one of them (A) actually persists for more than 1 km beyond the area shown in

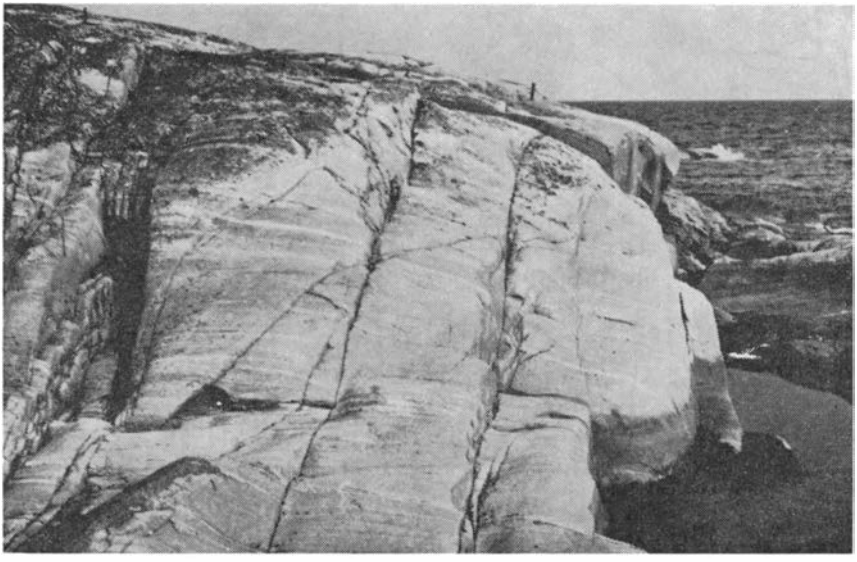

Fig. 2. Vertical joints of the E 35°S set. The joints at the centre are about 1 m apart.

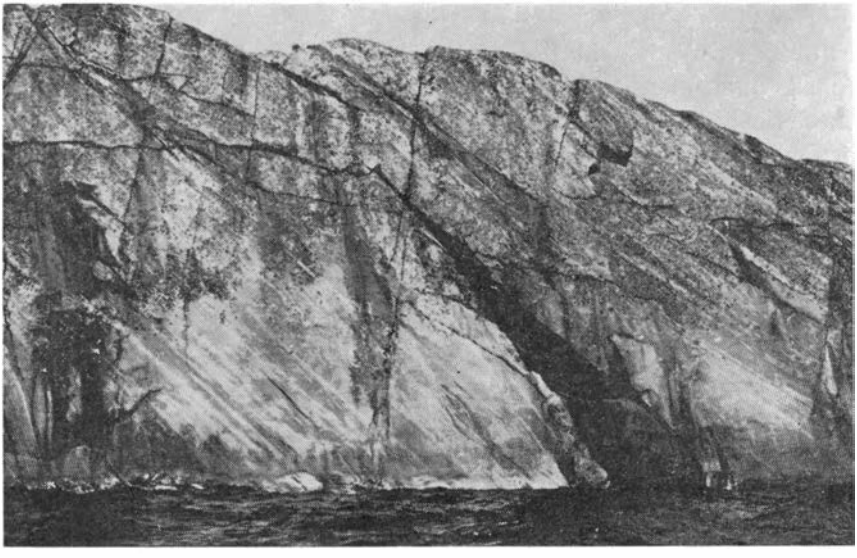

Fig. 3. Vertical rock wall about 10 m high, due to one of the E 35°S joints.

Fig. 1. These joints may possibly represent shear fractures due to a compression perpendicular to the strike, a final stage in the stress action which produced (or enhanced) the schistosity of the gneiss, though it must be admitted that the angle between them and the supposed stress direction is very small for such an interpretation. (Even if it is assumed that the stress was perpendicular to the main schistosity plane, i.e. inclined by about 45° from the horizontal, the real shear angle will not be very much greater, about 27°.) Presumably these joints are the older ones.

Approaching joint A (Fig. 1) from the south, the joints of the E 35°S trend are seen to bend gradually so that at the contact they form an angle of about 70° with joint A. It should be noted that the strike of the gneiss is not influenced by this curving (Fig. 4). A curve which is everywhere parallel to these joints can be simulated by combining the directions of two joint systems, the one parallel to the general E 35°S trend, the other perpendicular to joint A. The effect of the latter clearly decreases with increasing distance from joint A; at distances exceeding 200 m, it is practically negligible. As the joints are nearly vertical, it is sufficient in a simple treatment to consider only the two dimensions in the horizontal plane.

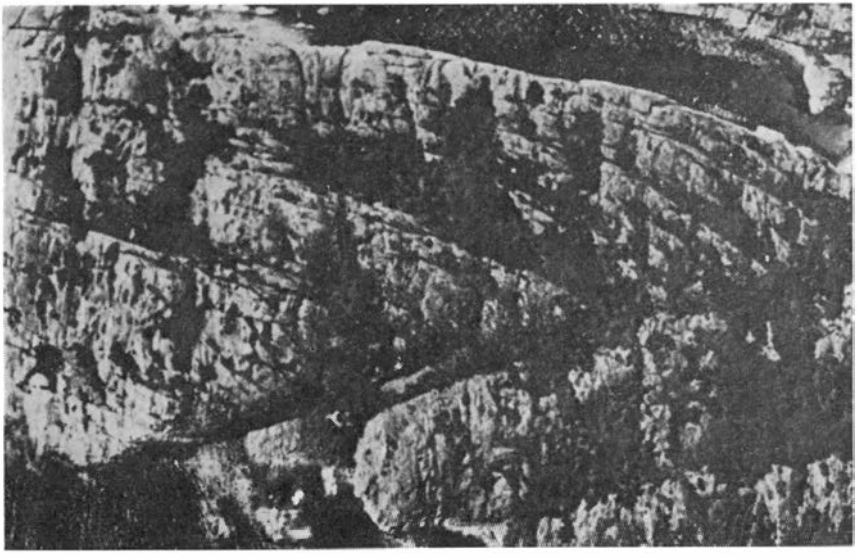

Fig. 4. Aerial photograph of curved joints. The area pictured is outlined in the upper left corner of Fig. 1. Photo: Nor Flyselskap.

Take the x-axis along the joint A and the y-axis perpendicular to it, the unit vectors $\mathbf{i}$ and $\mathbf{j}$ representing their directions. The constant (E 35°S) component is represented by the unit vector $\mathbf{j}_1$, which forms the angle α (about 70°) with $\mathbf{j}$. (Fig. 5). The other component is parallel to $\mathbf{j}$ and its magnitude depends on the distance, ξ, from the x-axis. Assuming this dependence to be exponential, the direction of the curve tangent at any distance from A is, in the simplest case, given by

$$\mathbf{r}^1 = \mathbf{j}_1 + e^{-\xi}\mathbf{j} = -\mathbf{i}\sin\alpha + \mathbf{j}(\cos\alpha + e^{-\xi}).$$

The curves themselves are then given by

$$\mathbf{r} = -\mathbf{i}(\xi + c_1)\sin\alpha + \mathbf{j}[(\xi + c_2)\cos\alpha - (e^{-\xi} + c_3)].$$

For the particular curve passing through the origin, c_1 and c_2 must be zero, and $c_3 = -1$:

$$\mathbf{r} = -\mathbf{i}\xi\sin\alpha + \mathbf{j}(\xi\cos\alpha - e^{-\xi} + 1).$$

This is equivalent to $x = -\xi\sin\alpha$ and $y = \xi\cos\alpha - e^{-\xi} + 1$, or

$$y = -x\cot\alpha - e^{x\operatorname{cosec}\alpha} + 1.$$

Inserting numerical values, α being chosen equal to 68°54′,

$$y = 1 - 0.386x - e^{1.07x}$$

For the relevant part of the curve, x is always negative. The Table shows some corresponding values. If the unit length is taken as 100 m, the curve conforms well to those formed by the joints, as shown in Fig. 5.

The tensions which produced these joints must be assumed everywhere normal to the tangent of the curve passing through the point in question. Their directions are then given by

$$\tan\varphi = \frac{\sin\alpha}{\cos\alpha + e^{-\xi}} = \frac{0.933}{0.360 + e^{-\xi}}$$

The angles φ corresponding to the listed values of ξ are shown in the last column of the Table; one instance is shown in Fig. 5.

The tension component parallel to x clearly has some relation to the gneiss body immediately beyond (north of) joint A. This body may have subsided rapidly along joint A, thus forming an approximately

Table

	Coordinates of curve through the origin		Direction of normal
ξ	x	y	φ
0	0	0	$34°27' = \frac{1}{2}\alpha$
0.1	−0.093	0.131	36°30′
0.2	−0.187	0.253	38°20′
0.3	−0.280	0.367	41°55′
0.4	−0.373	0.474	42°10′
0.5	−0.466	0.573	44°00′
0.7	−0.653	0.755	47°40′
1.0	−0.933	0.992	52°05′
1.5	−1.400	1.317	58°00′
2.0	−1.87	1.585	62°03′
2.5	−2.33	1.818	64°40′
3.0	−2.80	2.03	66°15′
∞	$-\infty$	∞	$68°54' = \alpha$

vertical, relatively rigid and cool boundary wall towards the hotter and more plastic gneiss at somewhat deeper levels. Plastic flow along A and along the strike at deeper levels, as well as contraction by cooling near the surface and near A, may have contributed to the formation of the joints and their curving as A is approached. It seems probable that the curved joints formed during a relatively short time interval, since the very special conditions required are not likely to persist for a long time in a gneiss area. Also, the temperature (and rigidity) at the boundary of the northern subsided gneiss body could not be maintained notably different from that of the southern gneiss in contact with it for any appreciable length of time. The existence of plastic flow at a suitable depth at the relevant stage is highly hypothetical, although it has been shown that some plastic deformation of the gneiss did occur at a very late stage (OFTEDAL 1956). Contraction by cooling is more easily visualized as a cause for the formation of the joints. The general E 35°S trend of the vertical joints is only locally and moderately modified by the extra cooling effect of the supposedly subsided gneiss body to the north.

To obtain a satisfactory agreement between the observed and calculated curving of the joints, it has been sufficient to take $e^{-\xi}$ instead

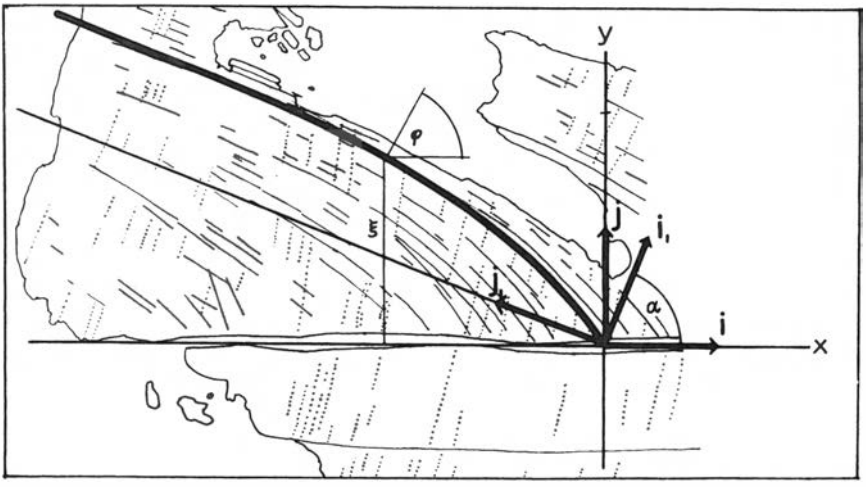

Fig. 5. The coordinate system with the principal unit vectors and a representative of the calculated curves, super-imposed on the joint pattern partly shown in Fig. 4. The length of the unit vectors is 100 m.

of $ke^{-\xi}$ in the above analysis. This seems to imply that the tensile force component parallel to $\mathbf{i}$ close to fault A and that parallel to $\mathbf{i}_1$, were of the same order of magnitude. If each of them is taken equal to 1, the resultant tensile force close to A will be $|\mathbf{i} + \mathbf{i}_1|$, or 1.65. Receding southwards from A, it will, naturally, decrease towards 1 as $|\mathbf{i}e^{-\xi} + \mathbf{i}_1|$. The effect of this may have been to start the formation of the joints close to A at the moment a force corresponding to the tensile strength of the gneiss which had been built up there, and make the fracturing proceed gradually therefrom. Within the direction field in question (between $\mathbf{i} + \mathbf{i}_1$ and $\mathbf{i}_1$), the gneiss appears to have behaved as a mechanically isotropic body.

REFERENCE

OFTEDAL, IVAR. 1956. Small scale tectonics in a South Norwegian gneiss complex. Norsk geol. tidsskr. 36: 151–155, 2 Pl.

Accepted for publication February 1966

A pillow lava locality in the Grong District, Norway

By

Ebbe Zachrisson

(Sveriges Geologiska Undersökning, Stockholm 50)

In the course of field work during the summer of 1963, well-preserved pillow lavas were found in the Caledonian of the Grong district (Fig. 1). Due to road-work, ice-scoured outcrops north of Solberg farm had been cleared of their moraine cover. Although no detailed mapping was carried out, exposures with pillow lava structures could be followed for at least 1 km along the road to the northeast where they are associated with more coarse-grained gabbroic rocks. At the road junction west of Solberg, fragmental rocks, apparently of pyroclastic origin, can be seen.

The pillows, the size of which varies from a few decimetres up to more than a metre, are closely packed. The contact between different pillows is clearly marked by a dark border zone ranging from one to a

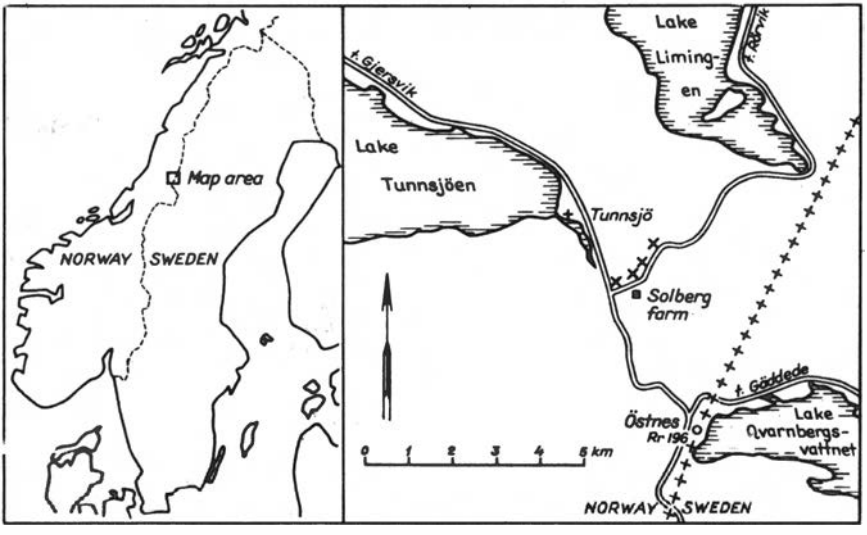

Fig. 1. Sketch map showing the localities of pillow lavas and pyroclastic rocks at the roadside near Solberg farm, Nord-Tröndelag, Norway.

Fig. 2. Pillows with thin border zones. Length of the compass about 12 cm. At the roadside NW of Solberg farm.

Fig. 3. Pillows with broad border zones. At the lower right corner, the vesicular texture is visible. Locality as Fig. 2.

few centimetres (see Figs. 2 and 3) in thickness. Generally, the interior of the pillow is lighter in colour, a little more coarse-grained and often shows an amygdaloidal structure. In thin sections, the rock is very fine-grained and mineralogical identifications are nearly impossible. X-ray diffractometer studies, however, point to a rather high content of amphibole (probably tremolite-actinolite), chlorite and plagioclase, some epidote, muscovite and calcite, and the presence of sphene. The quartz content is negligible, though some is present in calcite aggregates, which probably represent vesicular fillings. Apparently, the rock has a basaltic to andesitic composition.

Ever since REUSCH (1888) gave the first description of Caledonian pillow lavas (using the word 'ellipsoider') from the island of Bömmelöen (Bömlo) on the western coast of Norway, rocks of similar type have been reported from a great many places in the southern and middle part of the country (see VOGT 1946). As late as 1960, CARSTENS stated that 'pillow lavas ... have so far not been observed north and west of Steinkjer'. Generally, these volcanics are looked upon as belonging to the Stören Greenstones and thus assigned an Upper Cambrian to Lower Ordovician age.

From the Swedish part of the Caledonides, pillow lavas have been described from S. Storfjället in Västerbotten (BESKOW 1929) and from Låtats and Stuorab Titir in Norrbotten (KULLING 1948, KAUTSKY 1953). They have also been reported by Marklund from the Patta amphibolite southwest of Kebnekaise (see KULLING 1964).

Pillow lavas might have been observed in the Grong district by field geologists, but no mention of such structures is found in the literature dealing with the area. The well-preserved pillow lavas at Solberg, situated some 130 km northeast of Steinkjer, thus may be valuable when making stratigraphical correlations between this area and the Trondheim district, even if the stratigraphic position of such rocks in the Caledonides is a question that deserves further investigation.

REFERENCES

BESKOW, G. 1929. Södra Storfjället im südlichen Lappland. Sveriges geol. undersök. Ser. C, No. 350.

CARSTENS, H. 1960. Stratigraphy and Volcanism of the Trondheimsfjord Area, Norway. Norges geol. undersök. No. 212 b.

CHADWICK, B. *et al.* 1963. The Geology of the Fjeldheim—Gåsbakken Area. Sör-Tröndelag. Norges geol. undersök. No. 223.

KAUTSKY, G. 1949. Stratigraphische Grundzüge im westlichen Kambrosilur der skandinavischen Kaledoniden. Geol. Fören. Förh. Bd 71.

— 1953. Der geologische Bau des Sulitelma-Salojauregebietes in den nordskandinavischen Kaledoniden. Sveriges geol. undersök. Ser. C, No. 528.

KULLING, O. 1948. Om berggrunden i Sareks randområden. Geol. Fören. Förh. Bd 70.

— 1964. Översikt över norra Norrbottensfjällens kaledonberggrund. Sveriges geol. undersök. Ser. Ba, No. 19.

Norges Geologiske Undersökelse, 1958. Geologisk kart Tunnsjö, 1:100,000.

REUSCH, H. 1888. Bömmelöen og Karmöen med omgivelser. Kristiania (Oslo).

VOGT, TH. 1945. The geology of part of the Hölonda–Horg district. Norsk geol. tidsskr. 25.

— 1946. Vulkanismens faser i Trondheimsfeltet. Kgl. Norske Vidensk. Selsk. Forhandl. Bd 19. Trondheim.

Accepted for publication March 1966

Printed September 1966